Stress Analysis for the Hall D Tagger

Giangliang Yang
Glasgow University, January 2006

Abstract

A stress analysis for the Hall D Tagger magnet and vacuum chamber was performed by using Autodesk Inventor, which has a built-in finite element analysis program based on the commercial finite element analysis software ANSYS. The loads applied to the magnets are the magnetic force, the vacuum force between the magnet pole shoes and the weight of the magnet. When the magnet is running at 1.5 T, the magnetic force is around 150 tonnes, the vacuum force is around 30 tonnes and the magnet weights 40 tonnes. The calculated pole gap reduction is as small as 0.2 mm. A honeycomb structure is used to strengthen the vacuum chamber, and the load applied to the vacuum chamber is only the vacuum force. Stress analysis results show that, when the ribs are made from stainless steel with a section of 20mm *160 mm, the maximum deformation of the vacuum chamber along the exit window is around 1 mm. Due to the limitations of the software we used, all the above calculations are based on a single solid part model. From measurements on the Mainz tagger, the deflections calculated by using this method are underestimated by a factor of ~1.5.

1. Introduction

When the hall D tagger is running at 1.5 T, the magnetic force between a pair of pole shoes is around 150 tonnes. Additionally, because the pole shoes are acting as the lateral wall of the vacuum chamber, a significant vacuum force is applied to the magnet. Furthermore, the magnet weight is around 40 tonnes. All these forces tend to deform the magnet structures slightly, causing a small reduction in the pole gap and a small distortion in the field distribution. Since these deformations may have important effects on the mechanical and optical properties of the Tagger, it is advisable to do a stress analysis to calculate how the magnet body is deformed and then to estimate the effects.

The Hall D tagger needs a long vacuum chamber to provide vacuum protection for the electron trajectories being analysed. Basically, the vacuum chamber is a flat box, which is made from stainless steel of thickness 15 mm. The length of the vacuum box is around 12 m along the focal plane flange, and the maximum width in the middle of the box is around 0.9 m. The box also extends the vacuum from the magnet exit edges close to the focal plane. The focal plane flange has a very thin vacuum window, which should be thin enough to ensure multiple scatting of the electrons in the window is tolerable. To avoid introducing obstacles to the electrons, no internal supports are allowed inside the vacuum chamber. Since the vacuum chamber is not strong enough to support itself, it needs external supports. A honeycomb grid of ribs and some support arms which are attached to the magnet yokes are

designed to provide external support to the vacuum chamber. To check the feasibility of the supporting structure, a stress analysis was carried out.

For the stress analysis, ANSYS CAE (Computer-Aided Engineering) software was used in conjunction with Autodesk Inventor solid geometry to simulate the behaviour of a mechanical body under structural loading conditions. ANSYS automated FEA (Finite Element Analysis) technologies from ANSYS, Inc. generated the results listed in this report.

2. Stress analysis for the magnet body

A finite element mesh model is built based on the preliminary design of the hall D tagger magnets. Only one magnet is modelled due to similar loads applied to these two identical magnets. The mesh model contains 17854 nodes and 11033 elements. Because of the software's limited capability, the whole magnet is modelled as one solid part. The material used for the yoke and pole shoes is low carbon steel AISI 1006, which contains ~0.08% carbon. The mechanical properties of AISI 1006 are listed in table 1.

Table 1. Properties of AISI 1006

"AISI 1006" Properties

Name	Type	Value
Modulus of Elasticity	Temperature-Independent	190,000.0 MPa
Poisson's Ratio	Temperature-Independent	0.28
Mass Density	Temperature-Independent	7.86×10^{-6} kg/m m^3
Tensile Yield Strength	Temperature-Independent	285.0 MPa
Tensile Ultimate Strength	Temperature-Independent	330.0 MPa

All the loads and constraints are listed in table 2. The loads applied on the magnet are the magnetic attractive force between the pole shoes, vacuum forces and gravity. The magnetic force is the most important one. When the magnet is running at 1.5 T, the magnetic forces applied to a pair of pole shoes are around 150 tonnes. These forces are calculated by using Tosca by an integration of the Maxwell stresses over the relevant surfaces. Force 1" and 2" describe the magnetic forces applied to the top and bottom pole shoe surfaces, respectively. Because the pole shoe surfaces act as the lateral wall of the vacuum chamber, there are direct vacuum forces acting on the pole shoe surfaces. Pressure 1 and 2 indicate that 0.1 MPa vacuum pressures are present on the pole shoe surfaces. Since the vacuum chamber is not

strong enough to support itself, external support arms are used to strengthen it. These external vacuum support structures are connected to the magnet yoke. In the preliminary design, 6 support arms are used for the first magnet and 8 support arms are used for the second magnet. The forces applied to the magnet from these support arms are estimated to be 7.5 tonnes for each arm. Forces 3- 10 describe the forces present in these support arms. The last contribution to the structural loads is gravity. The finite element software calculated the weight of the magnet from the model volume and the material mass density. The gravitational constant g was taken as 9806.65 mm/s^2. Because the hall D tagger magnet is designed to rest on a three point supporting structure, the three supporting positions are used as fixed constraints to the model. Fixed constraints 1-3 in table 2 describe these constraints**.**

Figure 1 and figure 2 show the calculated stress and deformation for the magnet model. It can be seen that the maximum stress is around 15 Mpa and the maximum reduction in the pole gap is around 0.2 mm. Compared to the overall O-ring compression height of 6 mm, it is clear that this gap reduction will not affect the O-ring compression very much. Since the magnet pole gap is 3 cm, magnet pole gap, the 0.2 mm gap reduction is only 0.7 % of the pole gap and hence the effect on the magnet field will be small. Ideally, a further finite element calculation should be done by taking account this pole gap reduction to see if there is any effect on the Tagger optics. It also can be seen for Fig 2, that the maximum deformation of the bottom yoke is only around 0.02mm. This is clear evidence that the magnet is sufficiently stiff, and it can support itself.

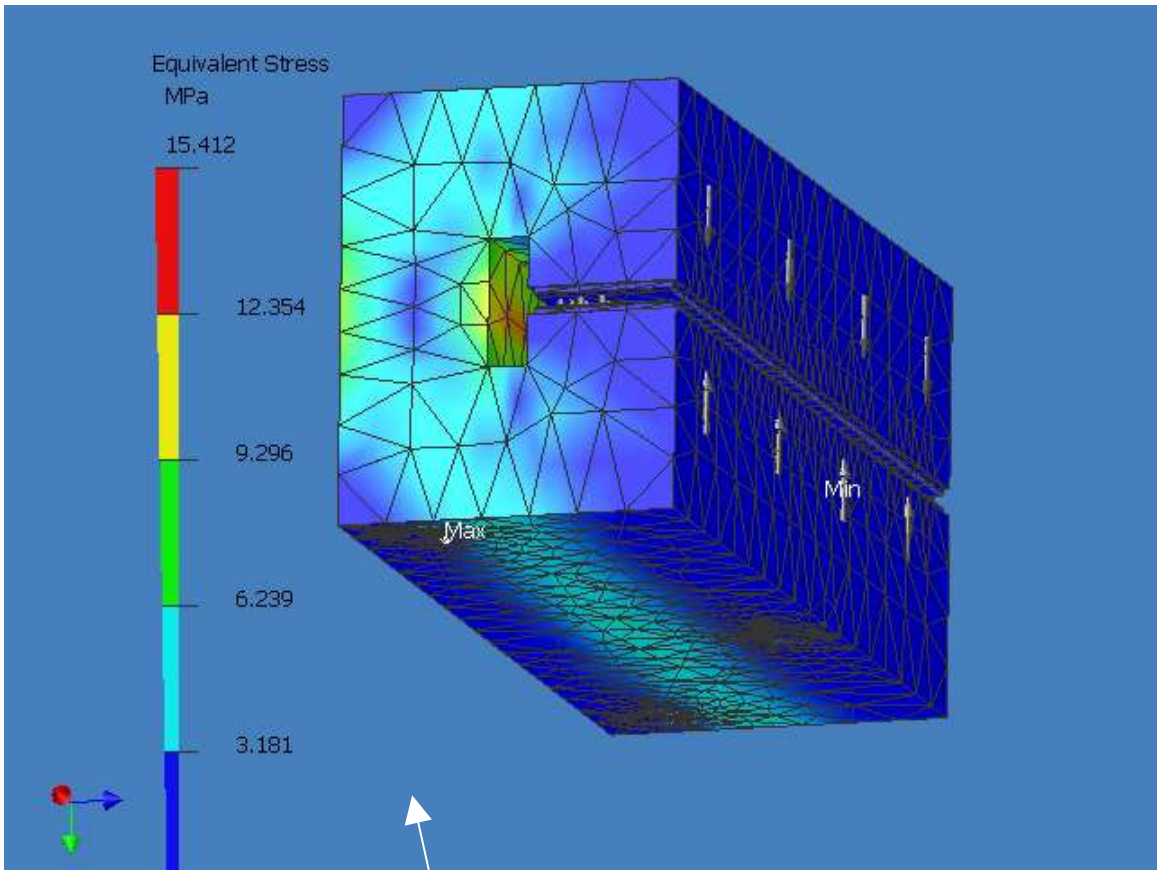

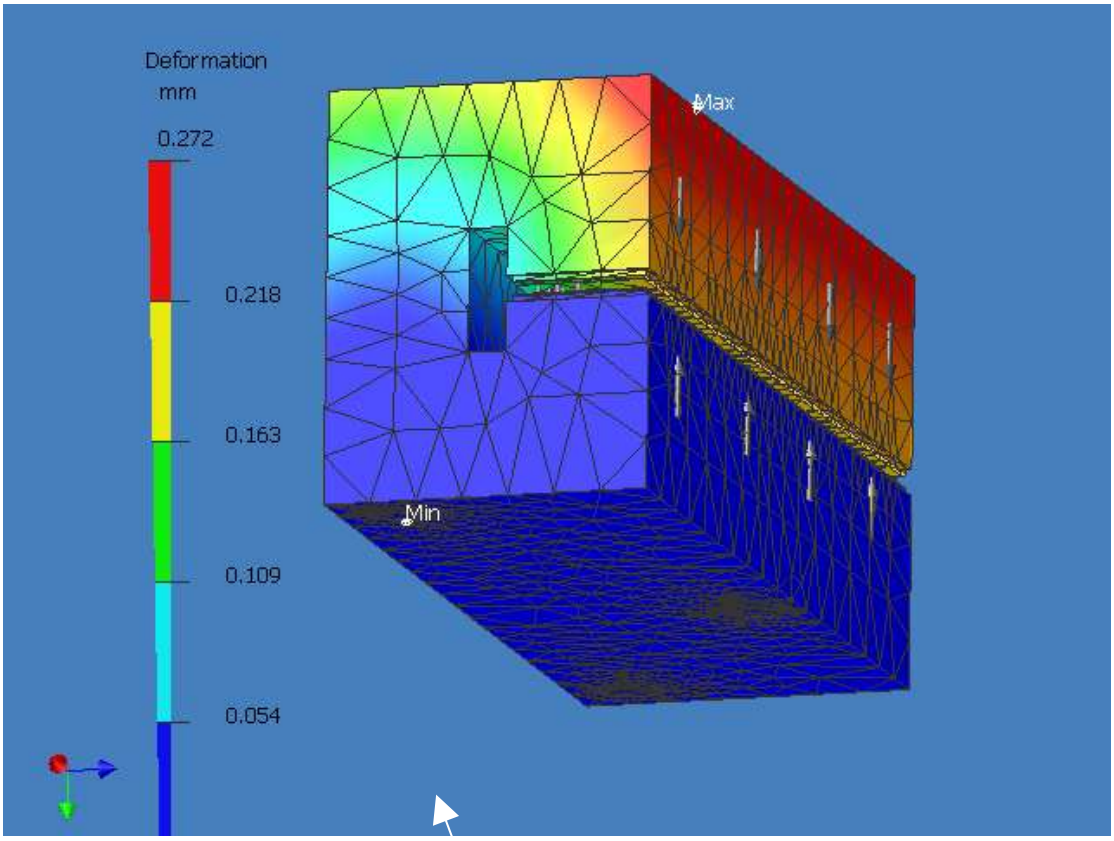

Fixed constraints

Figure 1. Equivalent stress result of the magnet under all major forces

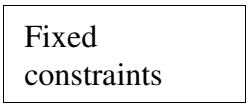

Figure 2. Deformation of the magnet under all major forces

Name	Type	Magnitude	Vector	Reaction Force	Reaction Force Vector	Reaction Moment	Reaction Moment Vector
"Force 1"	Surface Force	1.5×10⁶ N	[5.17×10⁻¹⁰ N x, 1.5×10⁶ N y, 9.49×10⁻²⁶ N z]	N/A	N/A	N/A	N/A
"Force 2"	Surface Force	1.5×10⁶ N	[5.17×10⁻¹⁰ N x, -1.5×10⁶ N y, 9.49×10⁻²⁶ N z]	N/A	N/A	N/A	N/A
"Force 3"	Surface Force	75,000.0 N	[0.0 N x, 75,000.0 N y, 0.0 N z]	N/A	N/A	N/A	N/A
"Force 4"	Surface Force	75,000.0 N	[0.0 N x, 75,000.0 N y, 0.0 N z]	N/A	N/A	N/A	N/A
"Force 5"	Surface Force	75,000.0 N	[0.0 N x, 75,000.0 N y, 0.0 N z]	N/A	N/A	N/A	N/A
"Force 6"	Surface Force	75,000.0 N	[0.0 N x, 75,000.0 N y, 0.0 N z]	N/A	N/A	N/A	N/A
"Force 7"	Surface Force	75,000.0 N	[0.0 N x, -75,000.0 N y, 0.0 N z]	N/A	N/A	N/A	N/A
"Force 8"	Surface Force	75,000.0 N	[0.0 N x, -75,000.0 N y, 0.0 N z]	N/A	N/A	N/A	N/A
"Force 9"	Surface Force	75,000.0 N	[0.0 N x, -75,000.0 N y, 0.0 N z]	N/A	N/A	N/A	N/A
"Force 10"	Surface Force	75,000.0 N	[0.0 N x, -75,000.0 N y, 0.0 N z]	N/A	N/A	N/A	N/A
"Pressure 1"	Surface Pressure	-0.1 MPa	N/A	N/A	N/A	N/A	N/A
"Pressure 2"	Surface Pressure	-0.1 MPa	N/A	N/A	N/A	N/A	N/A
"Fixed Constraint 1"	Surface Displacement	0.0 mm	[0.0 mm x, 0.0 mm y, 0.0 mm z]	122,320.17 N	[-4.36×10⁻⁴ N x, -122,320.17 N y, -4.35×10⁻⁴ N z]	1.4×10⁷ N mm	[1.4×10⁷ N mm x, 9.45×10⁻³ N mm y, 321,972.15 N mm z]
"Fixed Constraint 2"	Surface Displacement	0.0 mm	[- x, 0.0 mm y, - z]	140,782.33 N	[1.11×10⁻⁴ N x, -140,782.33 N y, -7.95×10⁻⁵ N z]	8.62×10⁶ N mm	[-8.61×10⁶ N mm x, -0.02 N mm y, -412,657.52 N mm z]
"Fixed Constraint 3"	Surface Displacement	0.0 mm	[- x, 0.0 mm y, - z]	94,266.46 N	[1.06×10⁻⁴ N x, -94,266.46 N y, -7.18×10⁻⁴ N z]	1.29×10⁷ N mm	[1.29×10⁷ N mm x, 0.03 N mm y, 130,303.63 N mm z]

Table 2 Structural Loads and *Constraint*

3. Stress analysis for the vacuum chamber.

The vacuum chamber will be built by using stainless steel. Its properties are shown in table 3. The mesh model contains 25241 nodes and 13762 elements. Apart from the vacuum chamber wall, a grid of ribs built using stainless steel with a section of 20mm*160mm is used to strengthen the vacuum chamber**.**

Table 3, Structural properties of stainless

Name	Type	Value
Modulus of Elasticity	Temperature-Independent	206,700.0 MPa
Poisson's Ratio	Temperature-Independent	0.27
Mass Density	Temperature-Independent	7.75×10^{-6} kg/mm^3
Tensile Yield Strength	Temperature-Independent	689.0 MPa
Tensile Ultimate Strength	Temperature-Independent	861.25 MPa

All the loads and constraints are shown in table 4. For simplicity, we ignore the weight of the vacuum chamber, so the vacuum force is the only load applied to the vacuum chamber, as indicated by "pressure 1" in table 4. The vacuum chamber has a planar symmetry and also the applied loads have the same symmetry, so the central plane of the vacuum chamber remains unchanged. In this situation, only half of the vacuum chamber needs to be modelled; and the central plane is used as a boundary, as indicated as "fixed constraint 1" in table 4. External supports have been used to strengthen the vacuum chamber. These are ribs and external arms. The ribs are built by using 20mm*160 mm stainless steel strips; they are equally spaced; the distance between the nearest two ribs is 190mm. The ribs and the vacuum chamber body are built into one solid structure. The external support arms are considered as fixed constraints to the model. In table 4, "fixed constraints 7-14" indicate the constraints applied by the support arms. The O-ring compression brackets are used to stop the vacuum chamber wall movement along the z direction. There are more than 30 brackets along the magnet exit edge for each magnet. Naturally, the connecting positions between the brackets and the vacuum chamber wall could be used as the constraints. But the large number makes this boundary condition too complicated. For simplicity, we used the vacuum chamber wall edge as a constraint since this will not introduce a large error. The fixed constraints 2-6 are the constraints applied by the O-ring seal compression brackets. In table 4, the reaction forces for each fixed constraint are also shown.

Figures 3 and 4 show the stress and deformation analysis results for the vacuum chamber. The maximum stress for the ribs is around 38 MPa. The maximum deformation is around 0.5 mm. Since this is only for half of the vacuum chamber, the total deformation will be around 1 mm. Compared to the 47mm vacuum gap of the vacuum chamber, such a deformation is acceptable.

Name	Type	Magnitude	Vector	Reaction Force	Reaction Force Vector	Reaction Moment	Reaction Moment Vector

"Pressure"	Surface Pressure	-0.1 MPa	N/A	N/A	N/A	N/A	N/A
"Fixed Constraint"	Surface Displacement	0.14 mm	[0.1 mm x, 0.1 mm y,0.0 mm z]	360,294.13 N	[8,185.54 N x, -410.78 N y, 360,200.9 N z]	7.61×10^{8} N mm	[7.51×10^{8} N mm x, -1.24×10^{8} N mm y, 3.02×10^{7} N mm z]
"Fixed Constraint 2"	Edge Displacement	0.0 mm	[- x, - y,0.0 mm z]	17,726.25 N	[4.97×10^{-8} N x, 3.17×10^{-8} N y, 17,726.25 N z]	900,944.44 N mm	[898,700.84 N mm x, 63,542.71 N mm y, -3.4×10^{-5} N mm z]
"Fixed Constraint 3"	Edge Displacement	0.0 mm	[- x, - y,0.0 mm z]	8,539.46 N	[-3.8×10^{-9} N x, 3.23×10^{-9} N y, 8,539.46 N z]	1.62×10^{6} N mm	[114,074.5 N mm x, -1.61×10^{6} N mm y, 2.39×10^{-6} N mm z]
"Fixed Constraint 4"	Edge Displacement	0.0 mm	[- x, - y,0.0 mm z]	48,300.68 N	[-2.42×10^{-8} N x, -6.73×10^{-8} N y, 48,300.68 N z]	2.55×10^{6} N mm	[2.54×10^{6} N mm x, 139,970.72 N mm y, -6.7×10^{-6} N mm z]
"Fixed Constraint 5"	Edge Displacement	0.0 mm	[- x, - y,0.0 mm z]	310.82 N	[1.24×10^{-8} N x, 1.55×10^{-8} N y, -310.82 N z]	256,986.79 N mm	[14,134.23 N mm x, -256,597.81 N mm y, 4.61×10^{-7} N mm z]
"Fixed Constraint 6"	Edge Displacement	0.14 mm	[0.1 mm x, 0.1 mm y,0.0 mm z]	10,636.44 N	[-8,185.54 N x, 410.78 N y, 6,779.52 N z]	1.22×10^{6} N mm	[66,703.7 N mm x, -1.21×10^{6} N mm y, -85,557.49 N mm z]
"Fixed Constraint 7"	Vertex Displacement	0.0 mm	[- x, - y,0.0 mm z]	15,630.95 N	[-5.43×10^{-10} N x, 1.58×10^{-9} N y, 15,630.95 N z]	0.0 N mm	[0.0 N mm x, 0.0 N mm y, 0.0 N mm z]
"Fixed Constraint 8"	Vertex Displacement	0.0 mm	[- x, - y,0.0 mm z]	22,082.5 N	[-4.01×10^{-9} N x, -7.67×10^{-9} N y, 22,082.5 N z]	0.0 N mm	[0.0 N mm x, 0.0 N mm y, 0.0 N mm z]
"Fixed Constraint 9"	Vertex Displacement	0.0 mm	[- x, - y,0.0 mm z]	50,890.58 N	[1.16×10^{-8} N x, -9.59×10^{-9} N y, 50,890.58 N z]	0.0 N mm	[0.0 N mm x, 0.0 N mm y, 0.0 N mm z]
"Fixed Constraint 10"	Vertex Displacement	0.0 mm	[- x, - y,0.0 mm z]	16,855.9 N	[-3.57×10^{-8} N x, -3.22×10^{-8} N y, 16,855.9 N z]	0.0 N mm	[0.0 N mm x, 0.0 N mm y, 0.0 N mm z]
"Fixed Constraint 11"	Vertex Displacement	0.0 mm	[- x, - y,0.0 mm z]	29,460.2 N	[1.42×10^{-8} N x, 3.83×10^{-8} N y, 29,460.2 N z]	0.0 N mm	[0.0 N mm x, 0.0 N mm y, 0.0 N mm z]
"Fixed Constraint 12"	Vertex Displacement	0.0 mm	[- x, - y,0.0 mm z]	27,159.51 N	[-7.82×10^{-10} N x, 3.16×10^{-8} N y, 27,159.51 N z]	0.0 N mm	[0.0 N mm x, 0.0 N mm y, 0.0 N mm z]
"Fixed Constraint 13"	Vertex Displacement	0.0 mm	[- x, - y,0.0 mm z]	24,858.43 N	[-1.06×10^{-8} N x, -1.04×10^{-8} N y, 24,858.43 N z]	0.0 N mm	[0.0 N mm x, 0.0 N mm y, 0.0 N mm z]

"Fixed Constraint 14"	Vertex Displacement	0.0 mm	[- x, - y,0.0 mm z]	61,493.17 N	[1.02×10^{-7} N x, 4.99×10^{-8} N y, 61,493.17 N z]	0.0 N mm	[0.0 N mm x, 0.0 N mm y, 0.0 N mm z]

Table 4. Structural loads and constraints.

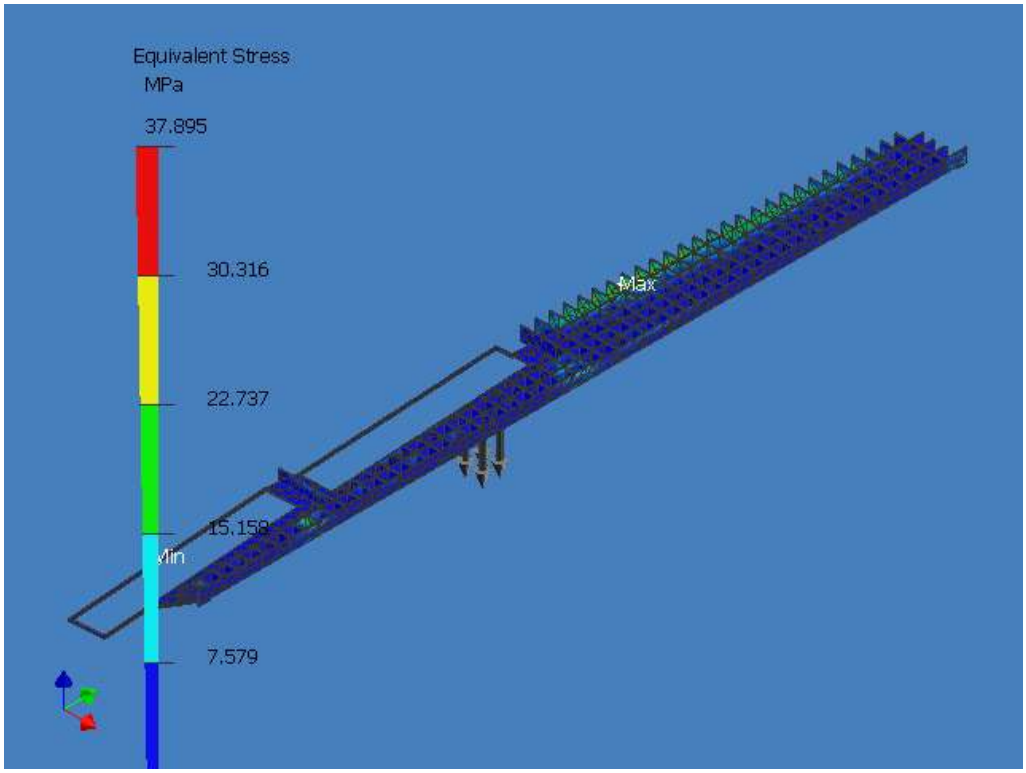

Figure 3: Equivalent stress for the vacuum chamber under vacuum forces.

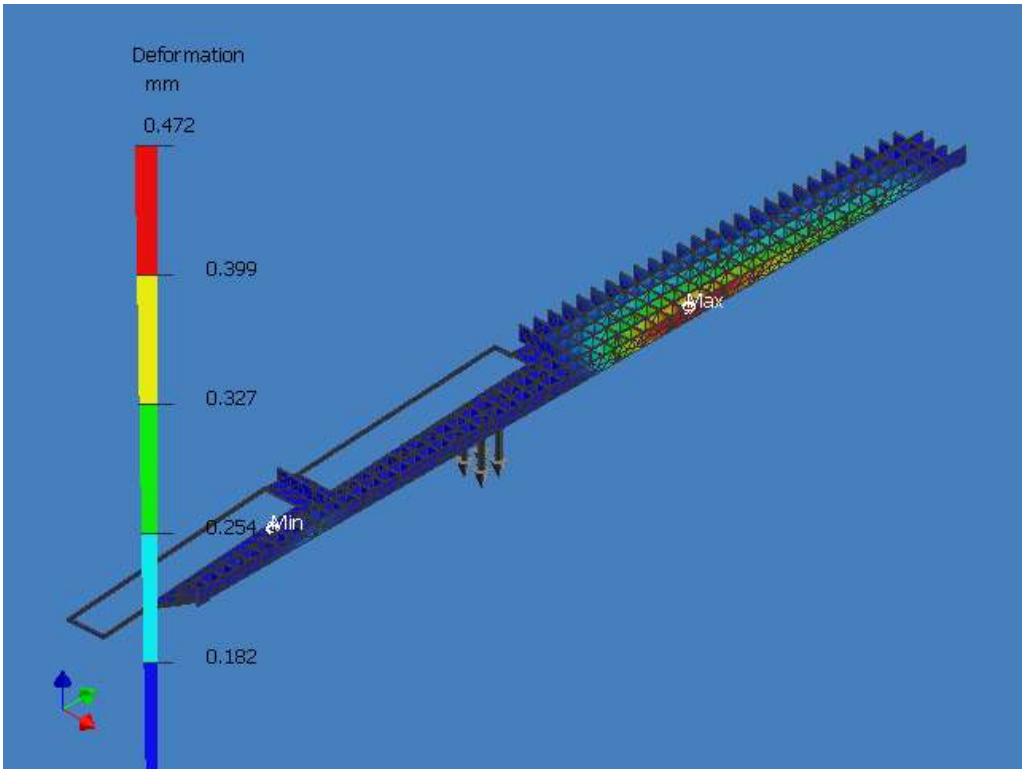

Figure 4: Deformation of the vacuum chamber.

4 Conclusion

Stress analyses have been done for the Hall D Tagger magnet and the vacuum chamber by using finite element software Autodesk Inventor 9. The gap reduction for the magnet is only 0.2 mm resulting from the magnetic attracting force, and various vacuum forces applied to the magnet. Compared with the 6 mm O-ring compression, this reduction is fairly small and will not cause any serious problems with the mechanical structure. However, further field calculations which take into account this small gap reduction should be done. A honeycomb grid rib structure is designed to strengthen the vacuum chamber. A finite element analysis shows that this ribs structure combined with external supporting arms and brackets will make the vacuum chamber sufficiently stiff to counteract the vacuum forces. The maximum deformation under such an arrangement is only 1 mm.